Electrification of Particles by Impact on Inclined Metal Plates

The electrification of particles falling onto metal surfaces was well correlated with the normal component of the impact velocity, showing that the electrification was mainly caused by the deformation of contact bodies. The current generated by the electrification at higher impact velocities was proportional to the velocity, while the current at lower velocities showed a different tendency. The elastic and plastic-elastic collision theory including particle roundness was used to explain these experimental results. Further, the coefficient of restitution, which was related to the work done by normal impulse, was determined by means of the velocity at the elastic limit obtainable from electrification data.

HIROAKI MASUDA
and
KOICHI IINOYA
Kyoto University
Kyoto 606, Japan

SCOPE

Particle electrification is of significant importance in powder handling processes. Electrification causes adhesion between particles and the wall of process equipment and brings about various undesirable effects. On the other hand, electrification has been used as a means of measuring powder flow rates and may also be applicable to particle characterization.

The electrification in gas-solids pipe flow has been studied with particular attention to the collision between particles and the pipe wall (Masuda et al., 1976), and it has been shown that the main factors affecting the electrification are the number of collisions and the area of contact. However, the effects of the particle velocity and the impingement angle have not yet been clarified.

In the present work, the electrification caused by the impact of falling particles on an inclined metal plate was studied both theoretically and experimentally. The current generated on the metal plate at various inclinations was measured for several kinds of metals and powders. The particle velocity was also measured. These data were examined in the light of the elastic and the plastic-elastic collision theory.

CONCLUSIONS AND SIGNIFICANCE

The present study confirmed that the electrification of particles by impact on an inclined metal plate was correlated with the normal component of the impact velocity. This result implies that the impact electrification arises mainly through deformation rather than friction. The theory based on the estimation of contact area successfully predicts the currents generated on metal plates. It was found that the currents at the elastic limit were less than those predicted by the elastic collision theory. Although the rebound of particles has a significant effect on various particulate processes, there have been no practical methods for estimating the coefficient of restitution. The impact velocity at the elastic limit, which is obtained from the data of currents, offers one possible means of estimating the coefficient.

It was also found that the currents generated on a virgin plate changed with the passage of time. Although the initial currents differed from point to point on the plate, the final values were the same and were reproducible. This fact must be taken into consideration in measuring the powder flow rate by use of the electric currents.

It was also confirmed that the currents were nearly inversely proportional to the particle diameter. The currents for smaller particles were larger than those predicted by neglecting the effects of roundness of particles. This tendency was also predicted successfully by the plastic-elastic collision theory.

AREA OF CONTACT

The electrification of particles takes place by charge transfer through the contact area. In estimating the variation of the electrification with the operating conditions of a particulate process, the contact area and the number of collisions are two important factors (Masuda et al., 1976).

When a particle impacts on metal with velocity v, contact region is compressed by the impactional force resulting in deformation over a certain area. After a short time, the particle rebounds because of the elasticity. Charge transfer between the materials proceeds during the very short time of contact.

When it is assumed that the particle is only elastically deformable, that the radius of curvature of the contact region does not change appreciably during the contact period, and that the angle ϕ in Figure 1 is zero, the con-

Correspondence concerning this paper should be addressed to Hiroaki Masuda.
0001-1541-78-1655-0950-$00.75.

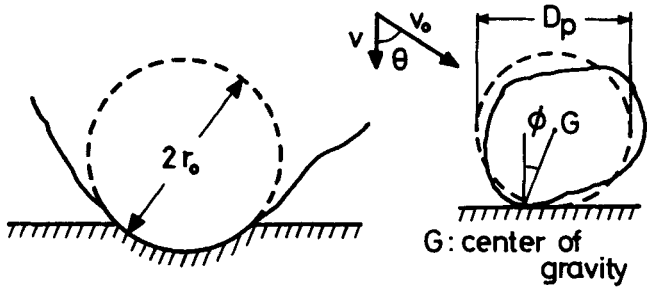

Fig. 1. Schematic diagram of impact.

tact area for the elastic collision is given from Hertz's theory (Timoshenko and Goodier, 1951; Bitter, 1963*a*) as follows:

$$S_e = \pi \left[\frac{3}{4} F_{\max} r_o \left(\frac{1-\nu_1^2}{E_1} + \frac{1-\nu_2^2}{E_2} \right) \right]^{2/3} \quad (1)$$

where $F_{\max}$ is given by

$$F_{\max} = \left(\frac{16}{9}\right)^{1/5} \left(\frac{5\pi}{3}\right)^{3/5} r_o^2 \left(\frac{1-\nu_1^2}{E_1} + \frac{1-\nu_2^2}{E_2} \right)^{-2/5} (\rho_p')^{3/5} v^{6/5}$$

$$= 3.02\, r_o^2 \left(\frac{1-\nu_1^2}{E_1} + \frac{1-\nu_2^2}{E_2} \right)^{-2/5} (\rho_p')^{3/5} v^{6/5} \quad (2)$$

Because the particle is nonspherical, the effective density ρ_p' is larger than ρ_p (Bitter, 1963*b*):

$$\rho_p' = \rho_p \, (D_p/2r_o)^3 = \rho_p \beta^{-3} \quad (3)$$

where

$$\beta = 2r_o/D_p \quad (4)$$

From Equations (1) through (4), the contact area for the elastic collision is given by

$$S_e = 1.36\, \rho_p^{2/5} \left(\frac{1-\nu_1^2}{E_1} + \frac{1-\nu_2^2}{E_2} \right)^{2/5} D_p^2 \beta^{4/5} v^{4/5}$$

$$= 1.31\, \rho_p^{2/5} E^{-2/5} D_p^2 \beta^{4/5} v^{4/5} \quad (\text{for } \nu_1 = \nu_2 = 0.3) \quad (5)$$

where

$$\frac{1}{E} = \frac{1}{E_1} + \frac{1}{E_2} \quad (6)$$

Hereafter the calculation is made for $\nu_1 = \nu_2 = 0.3$, for simplicity.*

At the elastic limit, the following relation is valid (Timoshenko and Goodier, 1951; Bitter, 1963*a*):

$$F_{\max} = \frac{2}{3} y S_e \quad (7)$$

From Equations (1) and (7), the maximum contact area by elastic deformation is given by

$$(S_e)_{\max} \equiv S_e^* = 0.51\, \pi y^2 D_p^2 \beta^2 E^{-2} \quad (8)$$

On the other hand, the area of contact by plastic deformation is derived in the same way as in the previous work (Masuda et al., 1976), except for the consideration of the radius of curvature r_o:

$$S_p = 2\pi r_o \sqrt{\frac{W_R}{\pi r_o y}} \quad (9)$$

W_R is represented by

$$W_R = \frac{1}{2} m_p (v - v_e)^2 \quad (10)$$

From Equations (9) and (10), the area of contact by plastic deformation is obtained as follows:

$$S_p = \pi D_p^2 \sqrt{\frac{\rho_p \beta}{6y}} (v - v_e)$$

$$= 0.41\pi D_p^2 \sqrt{\frac{\rho_p \beta}{y}} (v - v_e) \quad (11)$$

At the elastic limit $v = v_e$, the following relation is valid:

$$S_e(v_e) = S_e^* \quad (12)$$

Therefore, from Equations (5) and (8), the velocity at the elastic limit is given by

$$v_e = 1.29\, y^{5/2} \rho_p^{-1/2} \beta^{3/2} E^{-2}$$

$$= 1.29 \sqrt{\frac{y^5 \beta^3}{E^4 \rho_p}} \quad (13)$$

From Equations (8), (11), and (13), the area of contact for the plastic-elastic collision is represented by

$$S = S_e^* + S_p$$

$$= 0.41\pi D_p^2 \sqrt{\frac{\rho_p \beta}{y}} \left\{ v - 0.4 \sqrt{\frac{y^5 \beta^3}{E^4 \rho_p}} \right\}, \quad v > v_e \quad (14)$$

Moreover, the work done by the normal impulse is also represented by (Powell and Quince, 1972)

$$W_R = \frac{1}{2} m_p v^2 (1-e)^2 \quad (15)$$

From Equations (10) and (15), the coefficient of restitution is given by

$$e = \sqrt{1 - \left(\frac{v - v_e}{v} \right)^2} \quad (16)^*$$

CURRENT GENERATED ON METAL PLATE

From conservation of electric charge, the current generated on a metal plate is given by

$$I = -\frac{\Delta q}{m_p} W \quad (17)$$

The state of contact is represented by a parallel plate condenser with a gap of a few Angstrom units (Krupp, 1967) or by the contact transition region (Sze, 1969).†

Then Δq is represented by

$$\Delta q = \frac{\epsilon_o S}{z_o} V_c (1 - e^{-\Delta t/\tau}) \cong \frac{\epsilon_o S V_c \Delta t}{z_o \tau} \quad (18)$$

where $\epsilon_o S/z_o$ is the capacitance of the model condenser and must be replaced by $\epsilon S/z$ when the state of contact is represented by the contact transition region (Chowdry and Westgate, 1974).

* The Poisson ratios ν of most substances are between 0.2 and 0.4. Then the deviation of Se (ν_1, ν_2) from Se ($\nu_1 = 0.3$, $\nu_2 = 0.3$) is within the range of ± 3%.

* See also Appendix A for $\phi \neq 0$.

† This model is valid for insulators having traps uniformly distributed in the energy gap (Chowdry and Westgate, 1974).

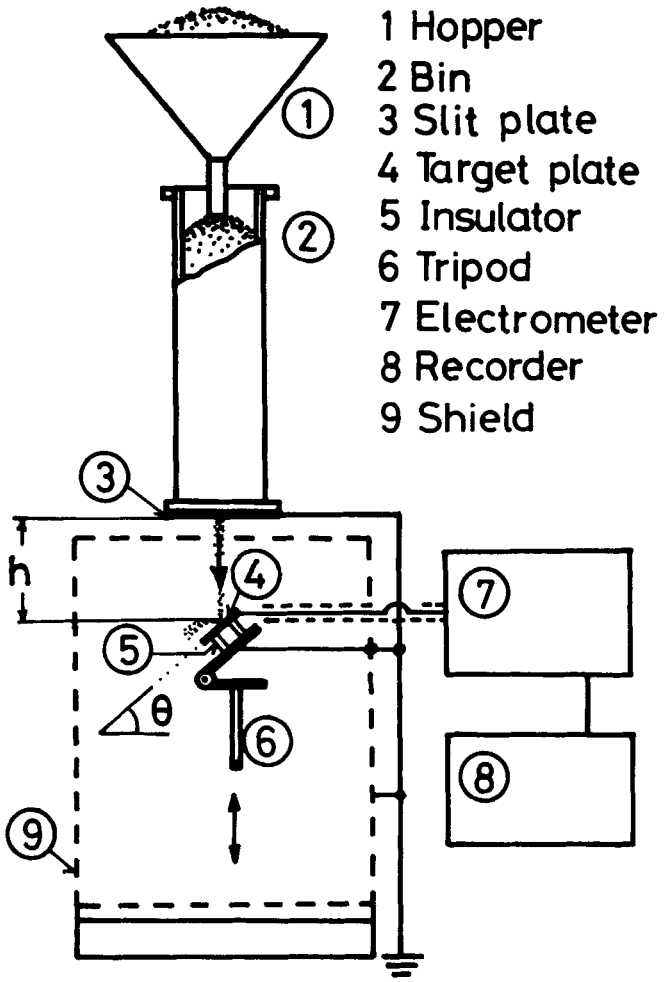

Fig. 2. Schematic diagram of experimental apparatus.

From Equations (5), (14), (17), (18), and the relation $v = v_o \cos\theta$, the current generated, is given by

$$I = -2.50 \frac{\epsilon_o V_c \Delta t W}{z_o \tau D_p} \left(\frac{\beta^4}{\rho_p^3 E^2}\right)^{1/5} (v_o \cos\theta)^{4/5},$$

$$v_o \cos\theta < v_e \quad (19)$$

$$I = -2.45 \frac{\epsilon_o V_c \Delta t W}{z_o \tau D_p} \sqrt{\frac{\beta}{\rho_p y}} (v_o \cos\theta - v^*),$$

Table 1. Powder Properties

Powder	Mass median diam., D_p [μm]	Geo. std. dev., σ_g	Mean particle diam.,* $\overline{D_p}$ [μm]	Density, ρ_p [g/cm^3]	β
Morundum					
(1)	55	1.3	48	3.97	0.20
(2)	71	1.1	64	3.97	0.16
(3)	93	1.1	84	3.97	0.11
(4)	120	1.2	100	3.97	0.11
(5)	180	1.2	149	3.97	0.14
(6)	290	1.1	264	3.97	0.12
(7)	450	1.1	409	3.97	0.09
(8)	660	1.1	599	3.97	0.07
Quartz sand	360	1.7	212	2.65	—
Glass beads	690	1.02	676	2.52	—

* $\overline{D_p} = 1 \Big/ \int \frac{f}{D_p} dD_p$.
f: particle size distribution.

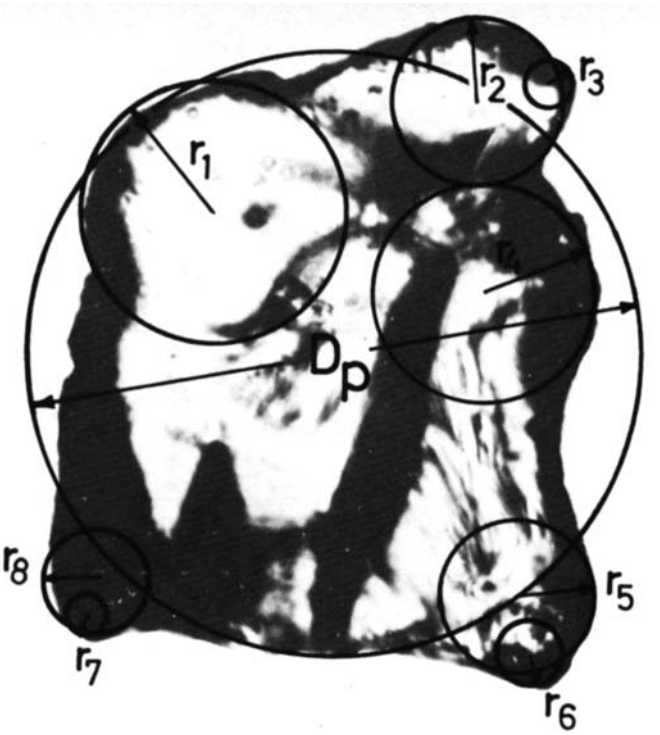

$$\beta = \frac{2(r_1 + r_2 + \cdots + r_8)}{8 D_p} = 0.22$$

Fig. 3. Particle shape [Morundum (2)].

$$v_o \cos\theta \geqq v_e \quad (20)$$

where

$$v^* = 0.04 \sqrt{\frac{y^5 \beta^3}{E^4 \rho_p}} \quad (21)$$

EXPERIMENTAL APPARATUS AND PROCEDURES

A schematic diagram of the experimental apparatus is shown in Figure 2. The level of powder in the bin was held constant. The bin, made from acrylic resin, was wrapped with aluminum foil and grounded. A copper plate with a slit was attached at the bottom of the bin, and it was also grounded. A metal target plate (3 cm × 10 cm) was electrically insulated with acrylic resins and fixed on a tripod. In connection with this, it is important to avoid the collision of particles with the acrylic insulator. Both the angle of inclination of the target plate and the distance between the slit and the target plate were adjustable.

The charges on particles falling from the slit or the target plate were measured with a Faraday cage. The current generated was measured with an electrometer (Takeda Riken Industry Co., Ltd., TR-8651). The measured values of the charges on unit mass of particles before and after impact and the current per unit mass flow rate of particles show that the charge was conserved.

In order to measure particle velocity, particles are sampled between $h - 1/2\ l$ and $h + 1/2\ l$. From material balance, the velocity v_o is given by

$$v_o = Wl/w \quad (22)$$

For accurate measurement, the sampling speed must be sufficiently high.

Powders used in the experiments are listed in Table 1. Morundum (aluminous abrasive) with various particle sizes are available on the market (product of Showa Denko Co.) fa-

TABLE 2. PROPERTIES OF METAL PLATES

Metal	Thickness, mm	Young's modulus,* E (dyne/cm^2)	Poisson's ratio*	Hardness,* Mohs	Work function,* (eV)
Al	1	7.1×10^{11}	0.34	2.9	4.25
Duralumin	1	—	—	2.95	—
Zn	1	$0.34 \sim 1.3 \times 10^{12}$	0.2 ~ 0.3	2.5	4.65
Cu	1	1.2×10^{12}	0.35	3.0	4.6 ~ 4.9
Brass	3	1.03×10^{12}	0.35	3 ~ 4	—
Fe	3	1.96×10^{12}	0.2	4.5	4.40
Stainless steel	0.8	—	—	—	—
Ni	1	2×10^{12}	0.3	—	4.96
Cr	1	—	—	9.0	4.37

* Kagaku-Binran, Maruzen, Japan (1966).

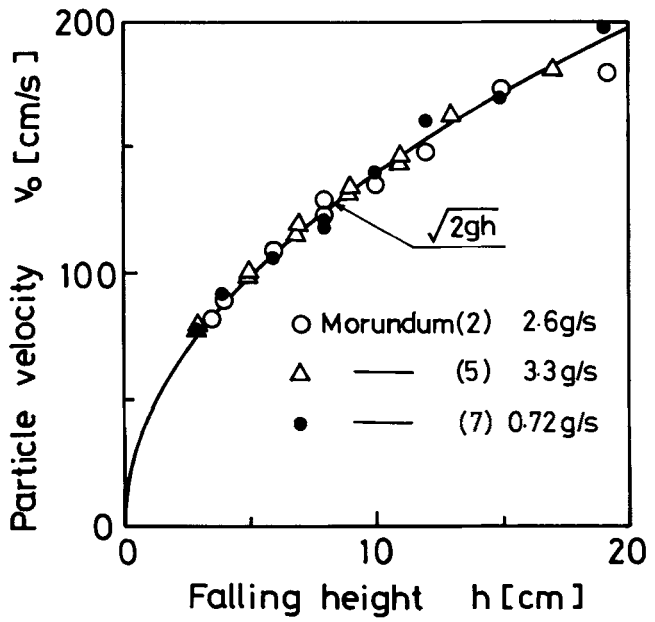

Fig. 4. Particle velocity v_0 as a function of falling height.

cilitating the study on effect of particle size. The values of β in the table were obtained from photomicrographs (Fig. 3). As the shape of the particle was not so extreme as a needle or disk, a falling particle would take random orientation, and, at the moment of impact, the convex region of the particle would contact with the metal plate. That is, all convex regions would have equal probabilities of contact. Therefore, radii of all convex regions (see Figure 3) were determined to get their arithmetic mean. Then the mean value was divided by the projected area diameter of the particle.

Metal plates tested in the experiments are listed in Table 2.

RESULTS AND DISCUSSION

Velocities of particles are shown in Figure 4 and are approximated by

$$v_o \cong \sqrt{2gh} \qquad (23)$$

The velocity of morundum (2) is higher than the terminal velocity. This may be explained by the cloud effect of falling particles (Boothroyd, 1971).

The current generated on a virgin plate changed with the passage of time as shown in Figure 5. Deformation hardening by particle impaction may be one of the causes of the change. The inversion of the polarity of the current shown in Figure 5*a* suggests the change of the composition of the surface material. The current, especially in the beginning, varied with the position on the target plate (see Figure 5*b*). This may derive from heterogeneous composition of the surface. However, the final values of

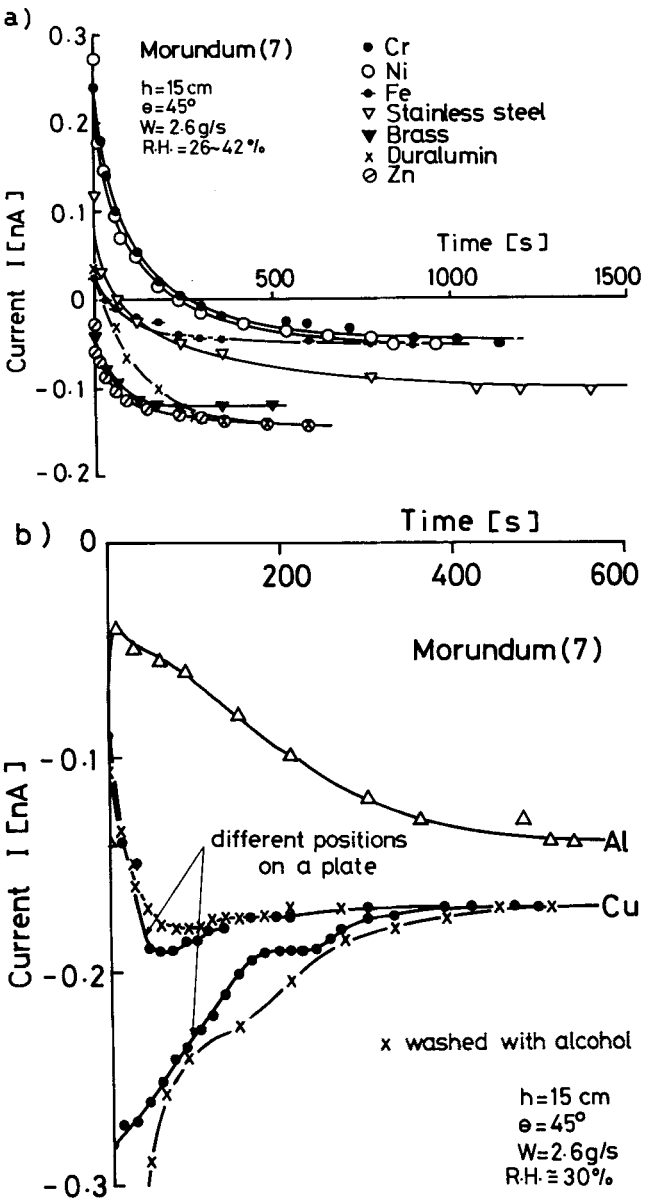

Fig. 5. Current generated on a virgin plate as a function of time.

the currents were the same and were reproducible. These tendencies did not change even after the surface was washed with alcohol. The surface was examined with a microscope and found to be aventurine with small scars. The stabilization times defined as the time that the current needs to reach within 5% of the final value are listed

Table 3. Stabilization Time of Current for Virgin Plates

Metal plate	t^*, s
Stainless steel	1 100
Cr	950
Ni	800
Fe	750
Zn	500
Al	500
Duralumin	350
Cu	350
Brass	250

h = 15 cm, θ = 45 deg, W = 2.6 g/s, morundum (7).

in Table 3, showing that a harder metal requires a longer stabilization time.

The steady state values of the currents generated by the impact of morundum (7) both on the copper plate and the stainless steel plate were obtained for various

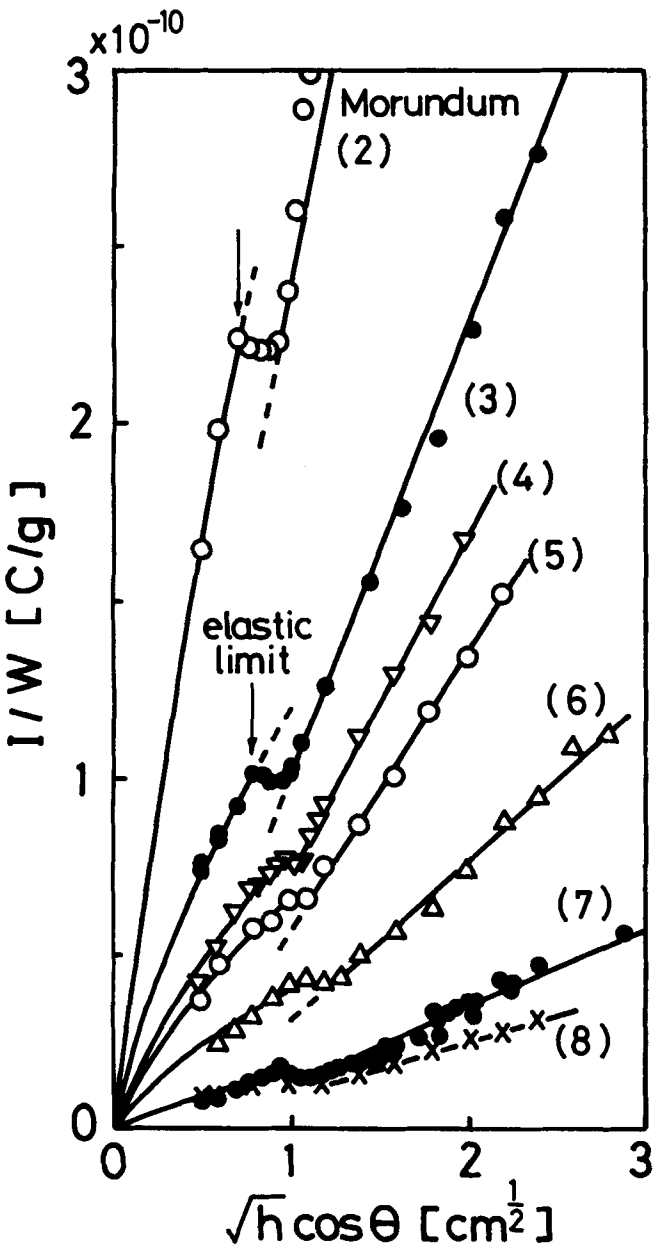

Fig. 6. Current per unit mass flow rate of powder vs. $\sqrt{h}\cos\theta$ (copper plate).

Table 4. v^* and v_e Obtained by Experiment

Metal plate	Powder	v^*, cm/s	v_e, cm/s
Stainless steel	Morundum (7)	27-33	70-80
	Glass beads	30	—
	Quartz sand	70	—
Cu	Morundum (1)	~0	40
	(2)	3	30
	(3)	9	35
	(4)	11	45
	(5)	12	45
	(6)	13	40-50
	(7)	17	42
	(8)	18	42

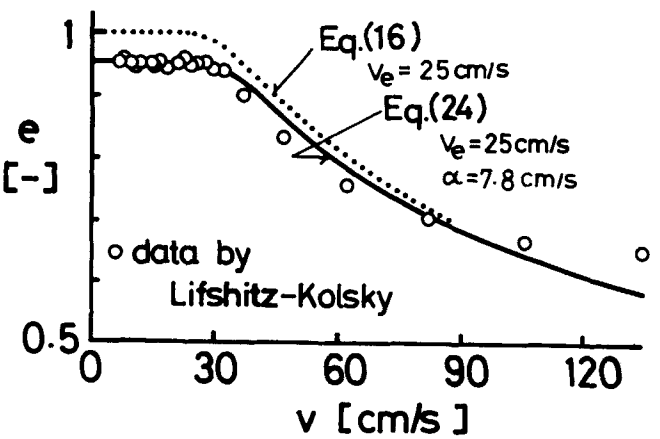

Fig. 7. Comparison between coefficient of restitution estimated and data obtained by Lifshitz and Kolsky.

falling heights h in the range from 2 to 20 cm and angles of inclination θ in the range from 20 to 75 deg. These data fall on the same line when they are plotted against $\sqrt{h}\cos\theta$, which is proportional to the normal component of the impact velocity. In the study on the kinetics of impact (Powell and Quince, 1972), it was shown that the energy dissipated by the normal impulse was correlated with the permanent deformations produced during the impact and that the energy dissipated by the frictional impulse was well correlated with the heating. The fact that the data obtained in this study were correlated with the normal component of the impact velocity implies that the impact electrification arises mainly through deformation rather than friction. This is in agreement with the experimental results of Ramer and Richards (1968), who found that electrification of sliding fabrics had no relationship to the coefficient of friction.† Figure 6 shows one of these results. Almost all of the data were well correlated with Equations (19) or (20), if we assume the constant value of $\Delta t/\tau$.†† However, the currents just after the elastic limit were less than those predicted by the elastic collision theory. This is due to aging of the target plate and may also depend on the surface properties of the plate. Further experiment will clarify this phenomenon.

The velocity v^* can be obtained from the point of intersection of the abscissa and the straight line. Also, the values of v_e were obtained from Figure 6 and are listed in Table 4. By use of v_e and Equation (16), the coefficient of restitution e may be approximately estimated. Figure 7 shows an example of the estimation. The data

† It has also been shown by Rose and Ward (1957) that a dielectric sphere can be charged by pure compression (without friction).

†† The mean value of $\Delta t/\tau$ in the region of elastic collision was 6.3 × 10^{-3}, while that in plastic-elastic collision was 6.2 × 10^{-3}, by use of typical value 3 × 10^{-6} C/cm^2 as $\varepsilon_0 V_c/z_0$.

Table 5. Current per Unit Mass Flow Rate

Powder	Plate	$I/W \times 10^{-10}$, C/g
Morundum (7)	Al	−0.58
	Duralmin	−0.51
	Zn	−0.49
	Cu	−0.48
	Brass	−0.41
	Stainless steel	−0.32
	Fe	−0.22
	Ni	−0.2
	Cr	−0.17
Glass beads	Stainless steel	−8.0
Quartz sand	Stainless steel	+0.21

h = 15 cm, θ = 45 deg, initial charge per unit mass of particles was $0 \sim -6 \times 10^{-11}$ C/g.

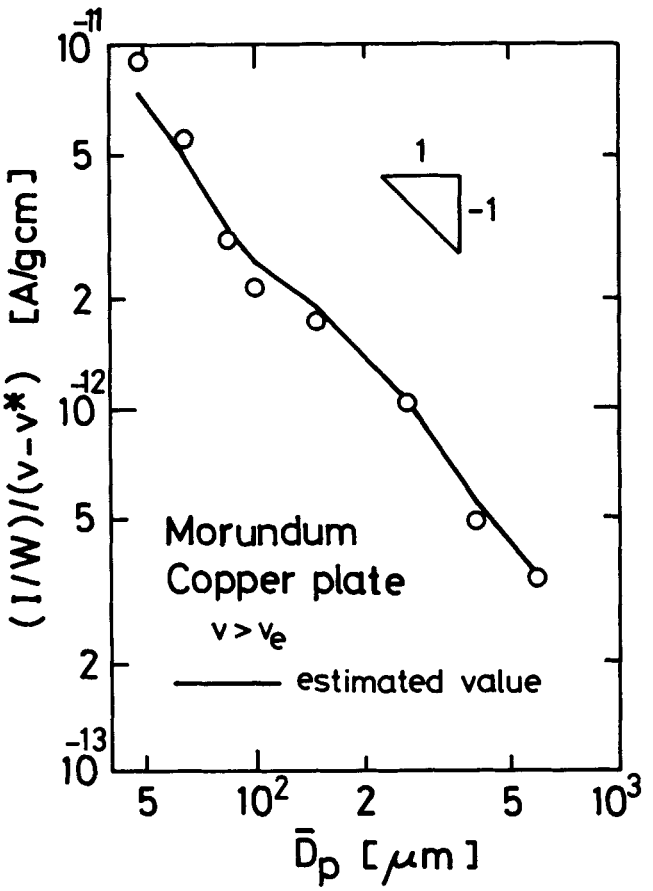

Fig. 8. Effect of particle size on generated current.

obtained by Lifshitz and Kolsky (1964) are for a large steel ball (12.7 mm in diameter), and e at the elastic limit is less than unity because of the local plastic deformation resulting from surface imperfections. To account for the energy loss due to the imperfections, Equation (16) is modified as follows:

$$e = \sqrt{1 - \left(\frac{v - v_e}{v}\right)^2 - \left(\frac{\alpha}{v}\right)^2} \qquad (24)$$

Results calculated by Equations (16) and (24) are shown in Figure 7 with dotted and solid lines, respectively. The trend of e against the velocity is well estimated by Equation (16) or (24).

It was also confirmed that the current was directly proportional to the powder flow rate W, provided W was relatively small. The currents per unit mass flow rate I/W are listed in Table 5, showing that values for the softer metals are larger. This fact coincides qualitatively with Equation (20), as the work functions of metals listed in Table 2 are almost the same.

The effect of the particle diameter on the currents is shown in Figure 8. The solid line was obtained from Equation (20) with the data for morundum (8) and the experimentally determined v^*. The line is not straight because of the effects of roundness of particles β and v^*.

ACKNOWLEDGMENT

The authors express their appreciation to Messrs. K. Fujii, T. Kouno, and Miss. A. Kobayashi for carrying out the experimental work.

NOTATION

D_p = particle diameter (diameter of a sphere having the same volume as the particle), cm
E_1, E_2 = Young's modulus of particle and plate, respectively, dyne/cm^2
E = $E_1 E_2/(E_1 + E_2)$
e = coefficient of restitution
F_{max} = maximum force at contact area, dyne
h = distance between slit and target plate, falling height, cm
I = current, A
l = height of sampling box opening, cm
m_p = mass of particle, g
q = charge on a particle, C
Δq = charge increment on particle by impaction, C
r_o = radius of curvature of a particle surface (see Figure 1), cm
S = area of contact, cm^2
S_e = contact area by elastic collision, cm^2
S_e^* = maximum contact area by elastic deformation, cm^2
S_p = contact area by plastic deformation, cm^2
Δt = effective duration of contact, s
V_c = contact potential difference, V
v = $v_o \cos\theta$, normal component of impact velocity, also referred to as impact velocity, cm/s
v_e = impact velocity at the elastic limit, cm/s
v_o = particle velocity, cm/s
v^* = velocity defined by Equation (21), cm/s
W = mass flow rate of powder, g/s
W_R = work done by normal impulse, erg
w = mass of particles sampled, g
y = yield pressure, dyne/cm^2
z = effective Debye length, cm
z_o = gap between contact bodies, cm

Greek Letters

α = constant in Equation (24) ($\frac{1}{2} m_p \alpha^2$ is the energy loss due to the imperfections), cm/s
β = $2r_o/D_p$, roundness of particle
ϵ_o = dielectric constant of air, F/cm
ϵ = dielectric constant of particle, F/cm
θ = angle of inclination of target plate, deg
ν_1, ν_2 = Poisson ratio of particle and plate, respectively
ρ_p = particle density, g/cm^3
ρ_p = $\rho_p \beta^{-3}$, effective particle density, g/cm^3
τ = time constant of model condenser, s
ϕ = angle shown in Figure 1, deg

LITERATURE CITED

Bitter, J. G. A., "A Study of Erosion Phenomena, Part I," *Wear*, 6, 5 (1963*a*).

———, "A Study of Erosion Phenomena, Part II," *ibid.*, 169 (1963*b*).

Boothroyd, R. G., *Flowing Gas-Solids Suspensions*, p. 24, Chapman and Hall, Ltd., London, England (1971).
Chowdry, A., and C. R. Westgate, "The Role of Bulk Traps in Metal-Insulator Contact Charging," *J. Phys. D.: Appl. Phys.*, 7, 713 (1974).
Krupp, H., "Particle Adhesion Theory and Experiment," *Advan. Collid Interface Sci.*, 1, 111 (1967).
Lifshitz, J. M., and H. Kolsky, "Some Experiments on Anelastic Rebound," *J. Mech. Phys. Solids.*, 12, 35 (1964).
Masuda, H., T. Komatsu, and K. Iinoya, "The Static Electrification of Particles in Gas-Solids Pipe Flow," *AIChE J.*, 22, 558 (1976).
Powell, F., and B. W. Quince, "The Kinetics of Impact in Drop-weight Experiments," *J. Phys. D.; Appl. Phys.*, 5, 1540 (1972).
Ramer, E. M., and H. R. Richards, "Correlation of the Electrical Resistivities of Fabrics With Their Ability to Develop and to Hold Electrostatic Charges," *Textile Research J.*, 38, 28 (1968).
Rose, G. S., and S. G. Ward, "Contact Electrification across Metal-Dielectric and Dielectric-Dielectric Interfaces," *Brit. J. Appl. Phys.*, 8, 121 (1957).
Sze, S. M., *Physics of Semiconductor Devices*, p. 90, Wiley, New York (1969).
Timoshenko, S. P., and J. N. Goodier, *Theory of Elasticity*, Chapt. 12, McGraw-Hill, New York (1951).

APPENDIX A: CONTACT AREA FOR $\phi \neq 0$

When the angle ϕ in Figure 1 is not zero, the equations in the text are replaced by following equations:

$$\rho_p' = \rho_p \beta^{-3} (\cos\phi)^2 \tag{A1}$$

$$S_e = 1.31\, \rho_p^{2/5} E^{-2/5} D_p^{2} \beta^{4/5} v^{4/5} (\cos\phi)^{4/5} \tag{A2}$$

$$v_e = 1.29\, y^{5/2} \rho_p^{-1/2} \beta^{3/2} E^{-2} (\cos\phi)^{-1} \tag{A3}$$

$$S = 0.41\, \pi D_p^2 \sqrt{\frac{\rho_p \beta}{y}} \left\{ v - \left(\frac{1.29}{\cos\phi} - 1.25 \right) \sqrt{\frac{y^5 \beta^3}{E^4 \rho_p}} \right\} \tag{A4}$$

$$W_R = \frac{1}{2} m_p v^2 (1 - e^2)/p \tag{A5}$$

p in Equation (A5) is defined by (Powell and Quince, 1972) as

$$p = 1 + \frac{d^2}{k_o^2} \sin\phi (\sin\phi + \mu \cos\phi) \tag{A6}$$

where, d = distance between center of gravity and contact point, $m_p k_o^2$ = moment of inertia, μ = dynamic coefficient of friction.

$$e = \sqrt{1 - p\left(\frac{v - v_e}{v}\right)^2 - p\left(\frac{\alpha}{v}\right)^2} \tag{A7}$$

$$v^* = \left(\frac{1.29}{\cos\phi} - 1.25 \right) \sqrt{\frac{y^5 \beta^3}{E^4 \rho_p}} \tag{A8}$$

Manuscript received October 11, 1977; revision received May 2, and accepted June 8, 1978.

Prediction of the Sorptional Equilibrium Relationship for the Drying of Foodstuffs

ENRIQUE ROTSTEIN

and

ALAN R. H. CORNISH

Plapiqui (Uns-Conicet), Bahia Blanca, Argentina

After existing correlations were reviewed to predict the equilibrium of foodstuffs with moist air, it was found that they were not adequate. A new equilibrium expression is presented on the basis of equal chemical potentials in the external and internal phases. The resulting equation can be used over most of the range of moisture contents of sugar based foodstuffs including the high moisture region; it also provides simple analytical expressions for the partial derivatives of moisture content with respect to temperature and to water vapor activity.

SCOPE

Many practical design problems, such as dehydration, packaging, and storage, arise when a foodstuff is removed from an equilibrium situation and is required to attain a new one.

To model the kinetics of the rate processes involved, an equilibrium relationship is required in order to relate foodstuff moisture content to air-water vapor activity and temperature. In addition, partial derivatives of moisture content with respect to the two independent variables are required. Attempts to obtain mathematical descriptions of the equilibrium relationship have followed two main directions. In one of these, use has been made of theoretical expressions developed for the adsorption of gas molecules on nonvolatile solid surfaces, while in the other, empirical or semiempirical equations have been fitted to experimental data. The theoretical expressions for the adsorption of gas molecules on nonvolatile solid surfaces are applicable only at very low moisture contents, where the cells are no longer acting as water reservoirs. Most of the expressions that have been proposed were summarized by Labuza (1974). With a few exceptions (Henderson, 1952; Filonenko and Chuprin, 1967), the studies have been confined to a particular temperature and do not contain temperature explicitly as an independent variable. The behavior of the partial derivatives has not been studied, and, in fact, only a few of the existing expressions enable partial derivatives with respect to temperature to be readily obtained.

Enrique Rotstein is currently Visiting Professor at the Department of Chemical Engineering and Materials Science, University of Minnesota, Minneapolis, Minnesota.
Alan R. H. Cornish is at the Imperial College of Science and Technology, London, England.

0001-1541-78-1682-0956-$01.35